The Extended Sampling Method for Inverse Biharmonic Scattering

General Ozochiawaeze[1] Isaac Harris[1]

[1] Department of Mathematics, Purdue University

Theory and Applications of Elliptic PDE
University of California, Irvine
August 17, 2026

Inverse Scattering: Can we find a hidden object from its echoes?

Instead of predicting how a known object scatters waves (**forward problem**), inverse scattering works in reverse: we measure scattered waves outside to reconstruct the shape, size, or material of a hidden obstacle.

Classical Wave Models

- **Acoustic:** Scalar pressure waves (Helmholtz equation)
- **Electromagnetic:** Vector fields (Maxwell's equations)
- **Elastic:** Navier equations in solids

Flexural Wave Model (This Work)

- **Physical System:** Transverse plate vibrations (Biharmonic wave operator $\Delta^2 - \kappa^4$)
- **Higher-Order:** Fourth-order PDE requiring two boundary conditions per edge (clamped/free)

Source: F. Cakoni, D. Colton, and H. Haddar, *Transmission Eigenvalues*, AMS Notices, October 2021.

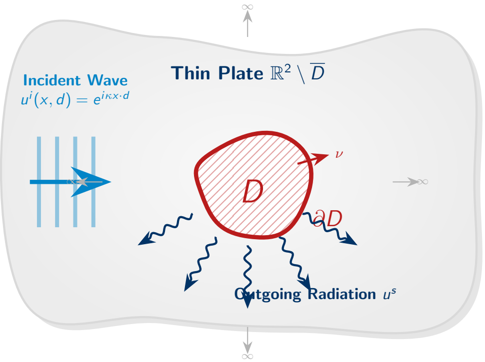

Biharmonic Wave Scattering Problem

Let $D \subset \mathbb{R}^2$ be a bounded clamped obstacle with smooth boundary ∂D. The scattered field satisfies

$$(\Delta^2 - \kappa^4)u^s = 0 \qquad \text{in } \mathbb{R}^2 \setminus \overline{D}.$$

Clamped boundary conditions:

$$u^s = -u^i, \qquad \partial_\nu u^s = -\partial_\nu u^i \qquad \text{on } \partial D.$$

Outgoing radiation:

$$\lim_{|x|\to\infty} |x|^{1/2}(\partial_{|x|} u^s - i\kappa u^s) = 0.$$

and

$$\lim_{|x|\to\infty} |x|^{1/2}(\partial_{|x|} \Delta u^s - i\kappa \Delta u^s) = 0.$$

Outgoing energy propagation.

Well-Posedness of the Forward Problem

Consider the clamped plate scattering problem

$$(\Delta^2 - \kappa^4)u^s = 0 \quad \text{in } \mathbb{R}^2 \setminus \overline{D},$$

with

$$u^s = -u^i, \qquad \partial_\nu u^s = -\partial_\nu u^i \quad \text{on } \partial D.$$

Theorem (Bourgeois–Hazard, 2020)

For every $\kappa > 0$, the clamped plate scattering problem admits a unique outgoing solution

$$u^s \in H^2_{\mathrm{loc}}(\mathbb{R}^2 \setminus \overline{D}).$$

Moreover, the solution depends continuously on the incident field:

$$\|u^s\|_{H^2(B\setminus\overline{D})} \leq C\left(\|u^i\|_{H^{3/2}(\partial D)} + \|\partial_\nu u^i\|_{H^{1/2}(\partial D)}\right),$$

for $\overline{D} \subset B$ with $B = B(0,R)$ large enough ball.

Reference:

- L. Bourgeois and C. Hazard (2020), *On Well-Posedness of Scattering Problems in a Kirchhoff–Love Infinite Plate*, SIAM Journal on Applied Mathematics, 80(3), 1546–1566.

Far-Field Measurements & The Inverse Problem

The Asymptotic Profile (2D): Outside the obstacle D, the scattered field decays cylindrically as $r = |x| \to \infty$:

$$u^s(x, d) = \frac{e^{i\pi/4}}{\sqrt{8\pi\kappa}} \frac{e^{i\kappa r}}{\sqrt{r}} u_D^\infty(\hat{x}, d) + \mathcal{O}\left(r^{-3/2}\right)$$

Where $\hat{x} \in \mathbb{S}^1$ is the observation direction and $d \in \mathbb{S}^1$ is the incident direction.

Ideal Inverse Problem (Full Data)

Reconstruct ∂D assuming full multistatic knowledge of the far-field pattern:

$$u_D^\infty(\hat{x}, d) \quad \text{for } \textbf{all} \text{ pairs } (\hat{x}, d) \in \mathbb{S}^1 \times \mathbb{S}^1$$

▶ Mathematically rich but highly unpractical for real-world setups. Highly ill-posed.

Our Target Problem (Few Incident Waves)

Reconstruct ∂D from a **finite, minimal set** of incident waves:

$$d \in \mathbb{S}^1_{\text{inc}} = \{d_1, \ldots, d_{N_d}\} \subset \mathbb{S}^1$$

with N_d very small (e.g., $N_d = 1$).
▶ Highly ill-posed.

Theoretical Motivation (Schiffer's Problem): Can an obstacle be uniquely determined by a *single* far-field measurement for all observation angles?

Flexural Far Field = Acoustic Far Field

The biharmonic operator factors as

$$\Delta^2 - \kappa^4 = (\Delta - \kappa^2)(\Delta + \kappa^2).$$

$$u^s = u^s_{\mathrm{pr}} + u^s_{\mathrm{ev}},$$

where

$$u^s_{\mathrm{pr}} = -\frac{1}{2\kappa^2}(\Delta - \kappa^2)u^s, \qquad u^s_{\mathrm{ev}} = \frac{1}{2\kappa^2}(\Delta + \kappa^2)u^s.$$

These components satisfy

$$(\Delta + \kappa^2)u^s_{\mathrm{pr}} = 0, \qquad (\Delta - \kappa^2)u^s_{\mathrm{ev}} = 0.$$

Propagating part

$$u^s_{\mathrm{pr}} \sim \frac{e^{i\kappa r}}{\sqrt{r}} u^\infty_D(\hat{x}, d)$$

Carries the far-field pattern.

Evanescent part

$$u^s_{\mathrm{ev}} = \mathcal{O}(e^{-\kappa r})$$

Vanishes at infinity and contributes no far-field data.

$$u^\infty_D(\hat{x}, d) = u^\infty_{\mathrm{pr}}(\hat{x}, d)$$

Qualitative Methods in Inverse Scattering

Overview: Qualitative methods recover the unknown object directly without nonlinear optimization loops or initial guesses.

Spatial Grid Sampling via Indicator Function $W(z)$

Inside Target ($z \in D$)
$W(z) > 0$

Outside Target ($z \notin D$)
$W(z) = 0$

Key Characteristics:

- **Pros:** Non-iterative, robust to initial guesses.
- **Cons:** Dense multistatic data usually required.

Foundational Lit: Cakoni & Colton, *Qualitative Methods in Inverse Scattering* — Colton & Kress, *Inverse Acoustic & EM Scattering Theory* (2019)

Extended Sampling Method (ESM) – A Qualitative Method

The Concept: Scan the workspace with an artificial test disk $B_z = B(z, R)$ centered at a test point z using a **single** incident wave direction.

$B_z \cap D = \emptyset$

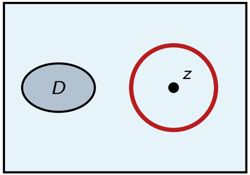

Indicator: $W(z) = 0$

$D \subset B_z$

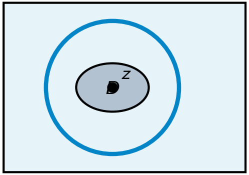

Indicator: $W(z) > 0$

- **Our Contribution:** Going beyond finding just the enclosing disk — we show we can recover **all** points z where $B_z \cap D \neq \emptyset$, enabling coarse support reconstruction for clamped biharmonic obstacles with sparse data.

Method Origin: J. Liu and J. Sun, Extended sampling method in inverse scattering, Inverse Problems, 34 (2018), 085007.

Identifiability from Far-Field Data

Theorem

Let $D_1, D_2 \subset \mathbb{R}^2$ be bounded scatterers. If their far-field patterns satisfy

$$u^{\infty}_{D_1} = u^{\infty}_{D_2} \neq 0,$$

then

$$\overline{D_1} \cap \overline{D_2} \neq \emptyset.$$

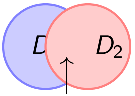

$\overline{D_1} \cap \overline{D_2} \neq \emptyset$

Goal

Construct an indicator $W(z)$ recovering sampling locations

$$\boxed{\{z : \overline{B_z} \cap \overline{D} \neq \emptyset\}}$$

from far-field data for a single wave.

Proof Idea:

- Rellich's lemma implies equality of far-field patterns gives equality of scattered fields outside both obstacles.
- If D_1 and D_2 were disjoint, unique continuation leads to a contradiction.

Auxiliary Probing Disk Sub-Problems

The Test Bed: To build our indicator, we model scattering by a canonical disk $B = B(0, R)$ under Helmholtz configurations with boundary states $\sigma \in \{\mathrm{Dir}, \mathrm{Neu}\}$:

$$(\Delta + \kappa^2)U_\sigma = 0 \quad \text{in } \mathbb{R}^2 \setminus \overline{B}, \qquad U_\sigma = U_\sigma^s + e^{i\kappa\hat{y}\cdot x}$$

Sound-Soft Probing ($\sigma = \mathrm{Dir}$)

Boundary setting: $U_{\mathrm{Dir}} = 0$ on ∂B.

$$U_{\mathrm{Dir}}^\infty(\hat{x}, \hat{y}) = \frac{4}{i}\left[\frac{J_0(\kappa R)}{H_0^{(1)}(\kappa R)} + 2\sum_{p=1}^{\infty}\frac{J_p(\kappa R)}{H_p^{(1)}(\kappa R)}\cos\left(p(\theta_{\hat{x}} - \theta_{\hat{y}})\right)\right]$$

- Smooth, analytically stable baseline.

Sound-Hard Probing ($\sigma = \mathrm{Neu}$)

Boundary setting: $\partial_\nu U_{\mathrm{Neu}} = 0$ on ∂B.

$$U_{\mathrm{Neu}}^\infty(\hat{x}, \hat{y}) = \frac{4}{i}\left[\frac{J_0'(\kappa R)}{H_0^{(1)\,\prime}(\kappa R)} + 2\sum_{p=1}^{\infty}\frac{J_p'(\kappa R)}{H_p^{(1)\,\prime}(\kappa R)}\cos\left(p(\theta_{\hat{x}} - \theta_{\hat{y}})\right)\right]$$

- Derivative-dependent normal fields.

These explicit analytical far-field kernels $U_\sigma^\infty(\hat{x}, \hat{y})$ form the integral kernels for our scanning operators.

Factorization & The Range Test Engine

The Probing Operator: Using the known analytical kernels U_σ^∞, we construct the **far-field operator** $F_{B_z}^\sigma : L^2(\mathbb{S}^1) \to L^2(\mathbb{S}^1)$ at spatial grid point z:

$$(F_{B_z}^\sigma g_z)(\hat{x}) = \int_{\mathbb{S}^1} e^{i\kappa(\hat{x}-\hat{y})\cdot z} U_\sigma^\infty(\hat{x},\hat{y}) g_z(\hat{y})\, ds(\hat{y})$$

If $-\kappa^2$ is not an interior Dirichlet/Neumann eigenvalue for Δ in B_z, then $F_{B_z}^\sigma$ is **injective, compact, and normal**.

Operator Factorization & Modified Far-Field Equation

Factors as $F_{B_z}^\sigma = -G_{B_z}^\sigma S_{B_z}^{\sigma *} G_{B_z}^{\sigma *}$ where $G_{B_z}^\sigma : H^{-1/2}(\partial B_z) \to L^2(\mathbb{S}^1)$ is defined by $G_{B_z} f = u_{B_z}^{\sigma,\infty}$ with $u_{B_z}^{\sigma,\infty} = U_\sigma$ when $f = -e^{i\kappa\hat{y}\cdot z}$. The range test relies on "solving" the compact operator equation:

$$(F_{B_z}^{\sigma *} F_{B_z}^\sigma)^{1/4} g_z = u_D^\infty(\cdot, d) \quad \text{(fixed incident direction } d\text{)}$$

Range Closure (Kirsch, 1998):

$$\text{Range}(G_{B_z}^\sigma) = \text{Range}\Big((F_{B_z}^{\sigma *} F_{B_z}^\sigma)^{1/4}\Big)$$

provided $-\kappa^2$ is not an interior Dirichlet/Neumann eigenvalue for Δ in B_z

Corollary:
$u_D^\infty(\hat{x}) \in \text{Range}\Big((F_{B_z}^{\sigma *} F_{B_z}^\sigma)^{1/4}\Big)$ iff:

$$\exists f \in H^{1/2}(\partial B_z) \text{ s.t. } u_{B_z}^{\sigma,\infty}(\hat{x}) = u_D^\infty(\hat{x}) \text{ only if } \overline{B_z} \cap \overline{D} \neq \emptyset$$

Main Result: The Picard Indicator Function

Theorem (Harris–O., 2026)

Let $\{\lambda_{z,\sigma}^{(j)}, \varphi_{z,\sigma}^{(j)}\}$ be the eigenpairs of the compact and normal $F_{B_z}^{\sigma}$. Assume $-\kappa^2$ is not an interior eigenvalue for B_z. Picard's criterion gives the indicator function:

$$W_\sigma(z; d) = \left[\sum_{j=1}^{\infty} \frac{\left| \langle u_D^\infty(\cdot, d), \varphi_{z,\sigma}^{(j)} \rangle \right|^2}{|\lambda_{z,\sigma}^{(j)}|} \right]^{-1}$$

Evaluating this across the workspace grid characterizes intersections:

$$W_\sigma(z; d) > 0 \implies \overline{B_z} \cap \overline{D} \neq \emptyset$$

▶ **Remark / Future Work:** Only sufficiency ($\implies$) is established here; currently unknown if the converse direction holds. Would like a complete characterization!

Geometric Localization: We can recover a coarse geometric surrogate of the hidden scatterer ∂D:

$$\partial D \approx \partial \{z : W_\sigma(z; d) > 0\}$$

Multiple Incident Directions & Radius Refinement

Directional Averaging: For a finite subset of incident angles, we accumulate indicators to achieve better reconstructions

$$\mathcal{W}(z) = \sum_{\ell=1}^{N_d} W_\sigma(z; d_\ell) \qquad \text{for } \ell \in \{1, 2, \dots, N_d\}$$

The Radius Bottleneck

The fidelity of the sampling boundary shape maps depends heavily on the chosen scale R:

- **Small** R **Limit:** Under-resolves components.
- **Large** R **Limit:** Causes over-smoothing.

Multi-Scale Solution

Introduce a geometric sorting refinement step:

$$R_p = \gamma^p R_0 \quad (\gamma > 1)$$

Stop when no 'artifacts' present in reconstruction
Empirical Observation: Best Radius:

$$R \sim \mathrm{diam}(D) \implies R_p \approx 0.5\,\mathrm{diam}(D)$$

Numerical Setup & Parameters

Configuration Summary:

- **Data Generation:** Synthetic far-field data for clamped biharmonic obstacles via boundary integral equations with noise model $u_\delta^\infty = u^\infty + \delta \cdot$ normalized noise.
- **Discretization:** $N = 32$ observation directions; sampling grid $[-4, 4]^2$ (tested 100 grid points).
- **Regularization:** Fixed parameter $\alpha = 10^{-4}$; radii sequence $R_p = (1.25)^p \cdot 0.5$.
- **Illumination:** Limited incident directions $N_{\text{inc}} \in \{1, 2, 4\}$ where $\mathbb{S}^1_{\text{inc}} = \{(\cos\phi, \sin\phi) : \phi = \frac{2\pi j}{N_{\text{inc}}}\}$.

Matrix Discretization ($N = 32$): The finite-dimensional matrix $\mathbf{F}_z^\sigma \in \mathbb{C}^{N\times N}$ is evaluated on equally spaced directions $\hat{x}_i = \hat{y}_i = (\cos\phi_i, \sin\phi_i)^\top$ via:

$$\mathbf{F}_z^\sigma(i,j) = \mathrm{e}^{-\mathrm{i}\kappa z\cdot(\hat{x}_i - \hat{y}_j)} U^\infty_{\sigma,B_0}(\hat{x}_i, \hat{y}_j), \quad i,j = 1,\ldots,N$$

where analytical kernels U^∞_{σ,B_0} are truncated to the first 11 Fourier modes ($n = 0,\ldots,10$).

Indicator Function on Test Grid (100×100): For N_{inc} incident directions $\{d_\ell\}$, we aggregate the spectral contributions using eigenvalue decomposition $\mathbf{F}_z^\sigma = \mathbf{V}_z\mathbf{\Lambda}_z\mathbf{V}_z^*$:

$$W_{\text{Recon}}(z) = \sum_{\ell=1}^{N_{\text{inc}}} \left[\sum_{j=1}^{N} \mathbb{1}_{[\alpha,\infty)}(|\lambda_j|)\,\frac{\left|u_\delta^\infty(\cdot\,, d_\ell)\cdot \mathbf{v}_z^{(j)}\right|^2}{|\lambda_z^{(j)}|}\right]^{-1}$$

with fixed threshold regularization parameter $\alpha = 10^{-4}$.

Numerical Example: Radius Scale Refinement

Reconstruction of a peanut-shaped obstacle centered at $(1, 1)$ (2% noise, $\kappa = 2$, 2 incident directions).

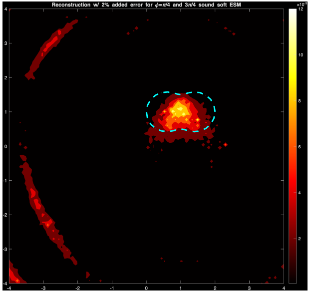

(a) Dirichlet: $R = 0.500$ ($p = 0$)

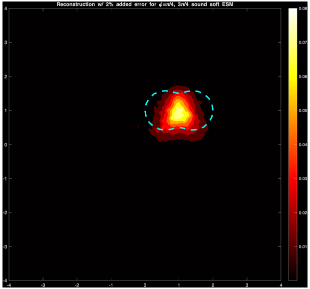

(b) Dirichlet: $R = 0.781$ ($p = 2$, Opt)

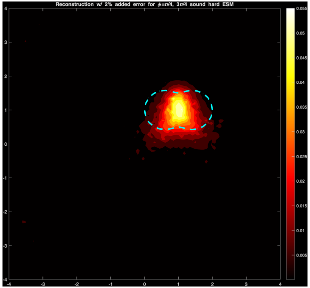

(c) Neumann: $R = 0.781$ ($p = 2$, Opt)

Numerical Inversions: Star-Shaped Obstacle

Reconstruction of a star-shaped obstacle centered at $(-1,-1)$ ($\kappa = \pi$, 10% noise, 4 incident directions $\mathbb{S}^1_{\text{inc},4}$).

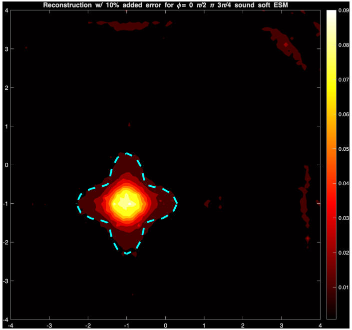

(a) $p = 3$; $R = 0.98$

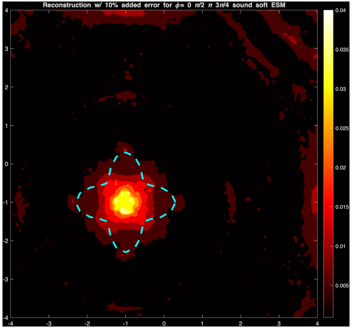

(b) $p = 4$; $R = 1.22$

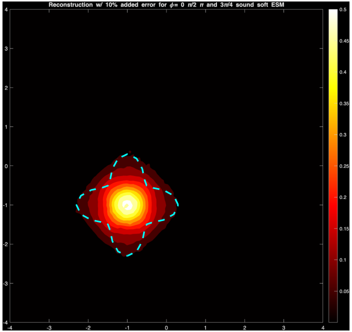

(c) $p = 5$; $R = 1.53$ (Opt)

Note: Increased incident illumination stabilizes reconstructions against high noise ($\delta = 0.1$).

Comparison: Sound-Soft vs. Sound-Hard

Star-shaped obstacle reconstruction ($\kappa = \pi$, 10% noise, 4 incident directions, optimal radius R).

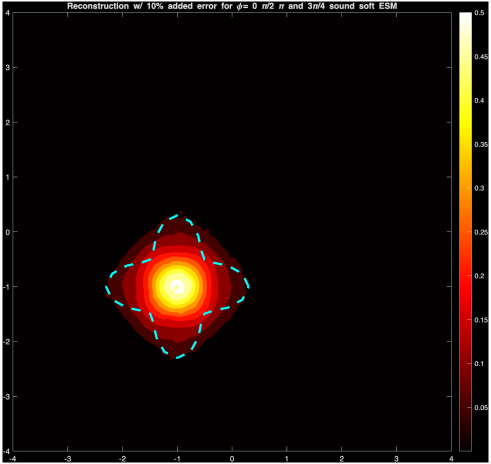

(a) Sound-Soft (Dirichlet)

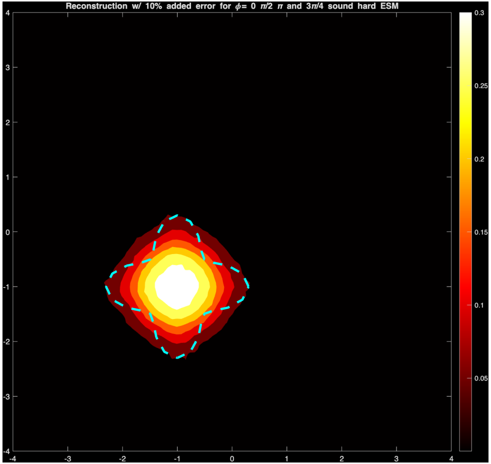

(b) Sound-Hard (Neumann)

Localizing via Imaging Functionals

Indicator Localization: $W_{\mathrm{Recon}}(z) = \|\mathbf{g}_z^\alpha\|_2^{-1}$ peaks at the optimal center $z^* = \arg\max W_{\mathrm{Recon}}(z)$ and empirically selected radius $R^* = R_p \approx 0.5 \cdot \mathrm{diam}(D)$ (no 'artifacts')

Peanut (Dirichlet, $\kappa = 2, \delta = 2\%$, 1 Inc)

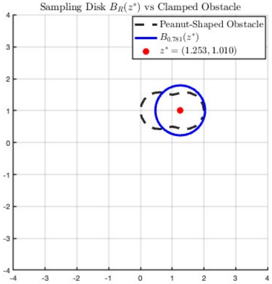

Star (Neumann, $\kappa = 2, \delta = 2\%$, 4 Inc)

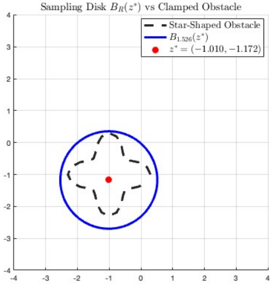

Reconstructed optimal disks $B_{R*}(z^*)$ successfully capture target support.

Key References I

I. Harris and G. Ozochiawaeze,
Novel implementation of the extended sampling method for inverse biharmonic scattering,
arXiv:2605.12367 [math.AP], 2026.

I. Harris, P. Li, and G. Ozochiawaeze,
Sampling methods for the inverse cavity scattering problem of biharmonic waves,
Inverse Problems, 42(1): 2026.

A. Kirsch,
Characterization of the shape of a scattering obstacle by the spectral data of the far field operator,
Inverse Problems, 14(6): 1489–1512, 1998.

A. Kirsch and N. Grinberg,
The Factorization Method for Inverse Problems,
Oxford University Press, 2008.